Direct test of the critical exponents at the sol-gel transition

Demet Kaya, Önder Pekcan, and Yaşar Yılmaz*
Department of Physics, Istanbul Technical University, Maslak, 34469 Istanbul, Turkey
(Received 10 March 2003; revised manuscript received 6 August 2003; published 29 January 2004)

The *steady state* fluorescence technique was used to study the sol-gel transition for the solution-free radical cross-linking polymerization of acrylamide (AAm), with N,N'-methylenebis (acrylamide) as cross linker in the presence of ammonium persulfate as an initiator. Pyranine (8-hydroxypyrene-1, 3,6-trisulfonic acid, trisodium salt) is used as a fluoroprobe for monitoring the polymerization. Pyranine molecules start to bind to acrylamide polymer chains upon the initiation of the polymerization, thus the spectra of the bonded pyranines shift to the shorter wavelengths. Fluorescence spectra from the bonded pyranines allows one to monitor the sol-gel transition, without disturbing the system mechanically, and to test the universality of the sol-gel transition as a function of some kinetic parameters such as polymer concentration, cross-linker concentration, and temperature. Observations around the critical point show that there are three regimes for AAm concentration in which the exponents differ drastically. The gel fraction exponent β and the weight average degree of polymerization exponent γ agree *best* with the static percolation results for higher acrylamide concentrations above $1M$, but they cross over from percolation to mean-field (Flory-Stockmayer) values when the AAm concentration is lower than $2M$. For very low polymer concentrations, below which the system can not form the gel, the exponents differ considerably from both the percolation and the mean-field values.

DOI: 10.1103/PhysRevE.69.016117 PACS number(s): 05.70.Jk, 64.60.Fr, 64.60.Ak

I. INTRODUCTION

The exact solution of the sol-gel transition was given first by Flory and Stockmayer [1,2] on a special lattice called a Bethe lattice on which the closed loops were ignored. An alternative to the chemical-kinetic theory is the lattice percolation model [3,4] where monomers are thought to occupy the sites of a periodic lattice. A bond between these lattice sites is formed randomly with probability p. For a certain bond concentration p_c, defined as the percolation threshold, the infinite cluster is formed in the thermodynamic limit. This is called the gel in polymer language. The polymeric system is in the sol state below the percolation threshold p_c.

The predictions of these two theories about the critical exponents for the sol-gel transition are different from the point of the universality. Consider, for example, the exponents γ and β for the weight average degree of polymerization D_w^{pol} and the gel fraction G (average cluster size S_{av} and the strength of the infinite network P_∞, in percolation language) near the gel point are defined as

$$D_w^{\mathrm{pol}} \propto (p_c - p)^{-\gamma}, \quad p \to p_c^-, \tag{1}$$

$$G \propto (p - p_c)^{\beta}, \quad p \to p_c^+, \tag{2}$$

where the Flory-Stockmayer theory the (so-called classical or mean-field theory) gives $\beta = \gamma = 1$, independent of the dimensionality d, while the percolation studies based on computer simulations give γ and β around 1.7 and 0.43 in three dimension [3–8].

These two universality classes for gelation problem are separated by a Ginzburg criterion [9] that depends upon the chain length N between the branch points as well as the concentration of the nonreacting solvent. The vulcanization of long linear polymer chains (large N) belongs to the mean-field class. Critical percolation (small N) describes the polymerization of small multifunctional monomers [3–6].

Some realistic features like multiple bonding, reversibility, and effect of solvent are generally not considered in static percolation [4]. By the computer simulation studies, Pandey *et al.* [10a] showed that the exponents γ and β (also, ν of correlation length exponent) change considerably for various solvent conditions, i.e., reversibility for physical gels, and the quality of solvent do affect the sol-gel transition. They also argued that [10b] the sol-gel transition for chemical gelation seems also nonuniversal with respect to quality of the solvent, degree of inhomogeneity depending on the quality of the solvent, and rate of reaction due to interplay between the phase separation and cross linking.

No real experiment measuring directly the critical exponents γ and β together with great sensitivity and accuracy has been performed so far, to our knowledge, at the sol-gel transition due to the experimental difficulties. Therefore, the result of the classical and percolation theories could not have been tested adequately with real experiments.

In order to understand the physical nature of polymerization processes underlying the transitions from the sol to the gel state, one must follow the reaction kinetics, and compare results with experiments directly measuring some physical properties in the course of the polymerization reaction. Experimental techniques used for monitoring this transition must be very sensitive to the structural changes, and should not disturb the system mechanically. Fluorescence technique is particularly useful for elucidation of detailed structural aspects of the gels. This technique is based on the interpretation of the change in anisotropy, emission and/or excitation spectra, emission intensity, and viewing the lifetimes of injected aromatic molecules to monitor the change in their microenvironment [11–14].

*Corresponding author. Email address: yyilmaz@itu.edu.tr

Fluorescence probes can be used in two ways for the studies on polymerization and gelation. First, one can add a luminescent dye as a probe to the system (extrinsic fluoruprobe). By using this fluoroprobe it is possible to measure some physical parameters of the polymerizing system, such as polarity [15,16], viscosity [17–20], and hydrofobicity [21]. In the second approach, the florophore is covalently attached to the polymer, and serves as a polymer-bond label (intrinsic fluoroprobe) [22], where the polymer fluoroprobe association depends on some factors including Coulombic interactions, the hydrophobicity of the polymer-florophore pair, etc.

These techniques have been successfully used to perform the experiments on polymerization [23,24], chemical gel formation [25–27], swelling of the gels [28], slow release of the probe molecules from gel [29,30], metal ion detection via metal ion templated polymeric gel [31], affinity of the gels to the target molecules [32], and examination of the collapsed state phases and volume phase transition of the polymeric gels [33]. These are all well-established methods.

Recent studies, using the pyrene as an extrinsic fluoroprobe, showed that the glass transition both for the linear bulk polymer [34] and gels [35] could be described by percolation exponents. In these studies, the fluoroprobe monitors the change occurring in the rigidity of the medium near the glass transition. Therefore, this method seems particularly suitable for studying the abrupt changes occurring during the glass transition of poly(methyl methacrylate) polymerization and/or gelation. As for the sol-gel transition, for either the solution polymerization or bulk polymerization, there are some difficulties to be overcome. For example, the probe can move randomly in the gel and be quenched by the sol molecules if the polymeric system is not in the glass state, therefore the intensity of the fluoroprobe will not be a direct function of the monomer conversion.

We surmount this difficulty and studied the free-radical cross-linking polymerization of acrylamide (AAm) using the pyranine (a derivative of the pyrene molecule, which has three functional groups on it [33]). The pyranine, added to the prepolymerization solution in very small amount, shows a spectral shift to the shorter wavelengths upon the initiation of polymerization. It is concluded that this spectral shift is due to the binding of pyranine to the polymer chains during the AAm polymerization. The pyranine, thus, becomes an intrinsic fluoroprobe while it is extrinsic at the beginning of the reaction. The total fluorescence intensity of the pyranine bonded to the strands of the polymers allows one to measure directly the average degree of polymerization and the gel fraction near the sol-gel transition, and thus the corresponding critical exponents γ and β.

II. EXPERIMENT

A. Materials

Gels were prepared by using various amounts of AAm (Merck) and various amounts of *N*,*N*-methylenebis (acrylamide) (BIS, Merck) by dissolving them in 25 cm^3 of water in which 10 μl of TEMED (tetramethylethylenediamine) were added as an accelerator. The initiator, ammonium persulfate (APS, Merck), was recrystallized twice from methanol. The initiator and pyranine concentrations were kept constant at $7\times10^{-3}M$ and $4\times10^{-4}M$, respectively, for all experiments. All samples were deoxygenated by bubbling nitrogen for 10 min, just before polymerization process.

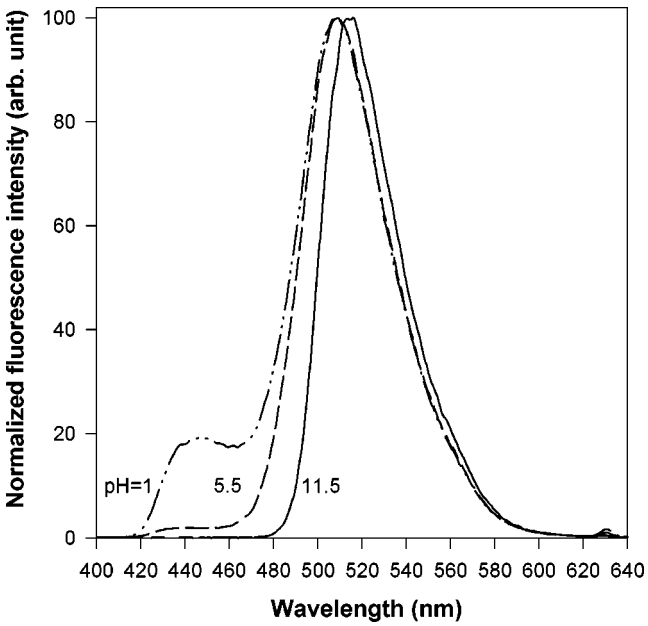

FIG. 1. Emission spectra of pyranine dissolved in pure water as a function of *p*H.

B. Gelation processes

First, the experiments of AAm with varying amounts (Table II), where the number of cross linker per AAm monomer was fixed, were performed at room temperature. Then, the experiments for different cross-linker contents (Table III) and different temperatures (Table IV) were repeated. The fluorescence intensity measurements were carried out using the Model LS-50 spectrometer of Perkin-Elmer, equipped with temperature controller. All measurements were made at 90° position and slit widths were kept at 5 mm. Pyranine was excited at 340 nm during *in situ* experiments and variation in the fluorescence spectra and emission intensity of the pyranine were monitored as a function of polymerization time.

III. RESULTS AND DISCUSSION

A. Prepolymerization experiments

Figure 1 shows the emission spectra of pyranine dissolved in pure water as a function of *p*H. At low *p*H, in addition to the main peak at 508 nm a small peak (like a shoulder) appears about 440 nm. After *p*H 6.5, this shoulder disappears and the 508-nm peak shifts to 512 nm. This figure indicates that the 440-nm peak corresponds to the neutralized pyranines by H^+ ions. In the whole range of *p*H, the ratio of the maximum intensities of the shoulder and the main peak, I_{440}/I_{508} does not exceed 0.2.

We have conducted some experiments for measuring the *p*H of the prepolymerization solution, and the results are summarized in Fig. 2. The *p*H of the prepolymerization so-

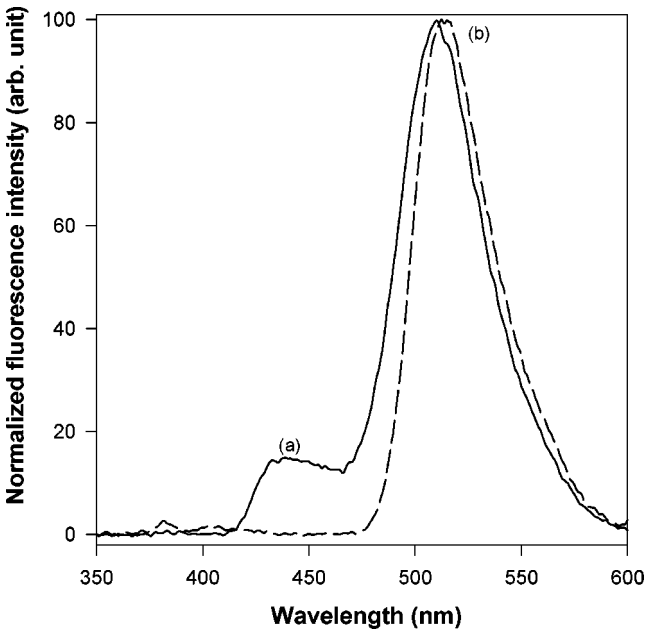

FIG. 2. Emission spectra of prepolymerization solutions, water-AAm-BIS-Pyranine (a) and water-AAm-BIS-Pyranine-TEMED (b).

lution, water-AAm-BIS-Pyranine was 6, thus 440-nm peak (the shoulder) appeared. Addition of TEMED to this led to an increase in the *p*H of the solution, from 6 to 8, and the shoulder disappeared as shown in Fig. 2. Addition of the initiator APS to the solution including TEMED did not lead to an extra change in the *p*H of the solution, it still remained 8.

No shift or change in the emission spectra of pyranine had been observed before the polymerization was initiated with APS. Upon the initiation of the polymerization the intensity of 512-nm peak started to decrease and a new peak appeared around 420 nm. Figure 3 shows a typical fluorescence spectra of pyranine at different stages of the AAm-BIS copolymerization. At the beginning of the reaction, only the 512-nm peak exists, then the intensity of the new (short-wavelength) peak started to increase as the intensity of the 512-nm peak (long-wavelength peak) decreased during the course of AAm polymerization.

Shift to the short wavelengths and increase in the intensity of short-wavelength peak during the polymerization should be due to the neutralization of SO_3^- groups of some of the pyranines in the reaction mixture. Therefore, the disappearing of the 512-nm peak at the end of the polymerization reaction, as shown in Fig. 3, can only be attributed to the binding of the pyranines to the poly(acrylamide) (PAAm) gel as previously observed by Yilmaz [33] for methacrylic acid co dimethyl(acrylamide) gels. The observations from Fig. 3 indicates also that the neutralization of the pyranine cannot be due to *p*H effect since the *p*H of the reaction did not change considerably during the polymerization.

To show that pyranine is really bonded to the gel, we conducted some swelling experiments. The final gels were brought to collapsed state and then put into pure water to swell. This process was repeated with fresh water a few times over weeks, and fluorescence measurements were performed, from time to time, on the gels during the swelling process. We observed only the short-wavelength peak from the washed gels, as shown in Fig. 4. This observation shows clearly the fact that pyranine is bonded to the gel during the polymerization process, since they still exist in the gel and have the short-wavelength spectra after the washing process was completed.

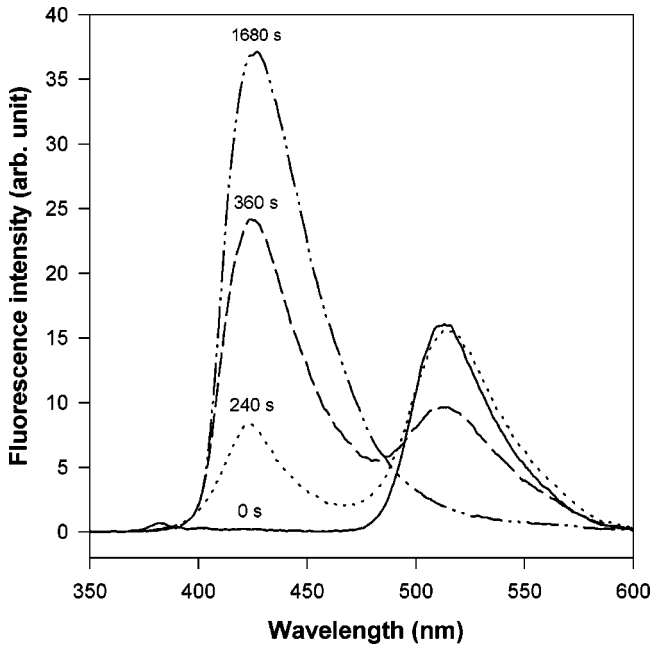

FIG. 3. Typical fluorescence spectra of pyranine at different stages during the AAm-BIS polymerization. Numbers on the spectra show corresponding reaction times.

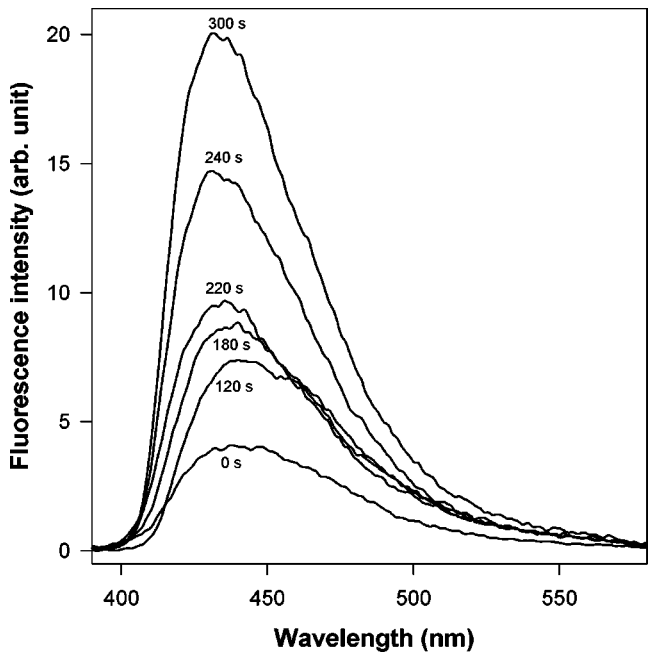

FIG. 4. Change in the fluorescence spectra of pyranine during the swelling of the AAm gels. The numbers on the curves represent corresponding reaction times.

The summary of the above paragraphs is that the charged and neutralized pyranine have two distinct spectra; the charged one corresponds to 512-nm peak at *p*H 8 (and 508 below *p*H 6.5) and the neutralized one corresponds to the peak around 420-nm wavelength. The neutralization of pyranine is due to the binding to the gel during polymerization. Pyranine was also used previously as a protein binding fluorescence dye. [36]

B. Gelation experiments

We have conducted the experiments for different AAm concentrations, cross-linker concentrations, and temperatures. Since 512-nm peak (corresponding to free pyranines in the sample cell) does not shift during the whole polymerization process, one may have a chance for real time monitoring of the polymerization by means of the change in the free pyranine intensity versus reaction time. Figure 5 shows the fluorescence intensity of the free pyranine from the reaction mixture as a function of the reaction time for different polymer concentrations, cross-linker concentration, and temperature.

As seen from the Fig. 5, the fluorescence intensity of the free pyranines first decreases rapidly to some value (initial stage of the polymerization; the region between *A* and *B* in the inset of Fig. 5), then starts to increase suddenly up to some point (gelation stage; *BC*), and again decreases to zero at the end of the reaction (final stage; *CE*). The same behavior in fluorescence intensity was also observed for different cross-linker contents [Fig. 5(b)] and different temperatures [Fig. 5(c)].

The decrease in the intensity of the initial stage depends on the polymer concentration, as the polymer concentration is increased the intensity decreases more and more. Besides, the amplitude of the peak (appeared in the gelation stage; *BCD*) changes depending on the polymer concentration. As the polymer concentration is increased from $0.5M$ to $5M$, the amplitude of the peak first increases to a maximum (at $2M$ AAm concentration) and then decreases for high polymer concentration [Fig. 5(a)].

For determining the gel points, each experiment was repeated at the same experimental conditions, and the gel points were determined by dilatometric technique [37]. A steel sphere of 4.8 mm diameter was moved in the sample up and down slowly by means of a piece of magnet applied from the outer face of the sample cell. The time when the motion of the sphere was stopped was evaluated as the onset of the gel point t_c. The t_c values are summarized in Table II, III, and IV, together with the other parameters. The gel points for densely formed gels (from $0.65M$ to $5M$, AAm concentrations) correspond to the times before the maxima of the peak (*BC*), and to the times after the maxima of the peak (*CE*) for the loosely formed gels (from $0.50M$ to $0.65M$, AAm concentrations).

The steel sphere in the samples of higher polymer concentration cannot be moved after the polymerization is completed, but it can partly be vibrated around its equilibrium position for the loosely formed gels, by moving the magnet up and down on the surface of the sample cell. Another observation was that below $0.5M$ polymer concentration, the polymeric system did not turn into gel; it remained as a viscous liquid.

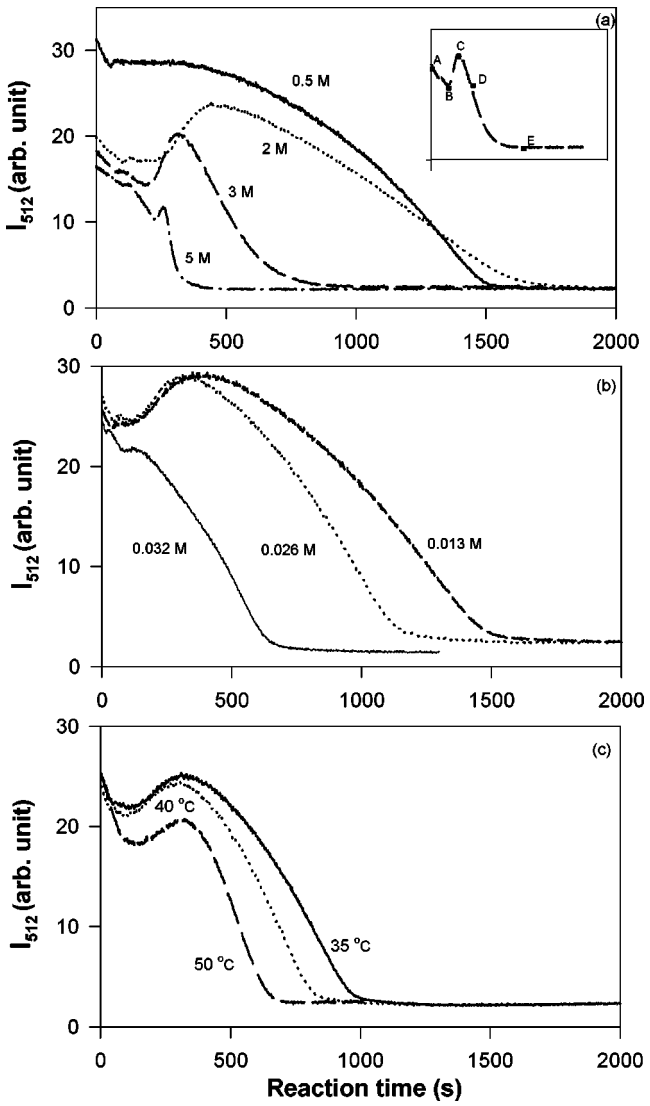

FIG. 5. Fluorescence intensity of the free pyranine at 512 nm I_{512} vs reaction time for varying AAm (a), cross-linker contents (b), and temperature (c). Numbers on curves indicate the AAm concentrations [for (a)], BIS contents [for (b)], and temperatures [for (c)]. The whole range of the variables is summarized in Tables II, III, and IV.

The probe molecule fluoresces at different wavelength only when it is incorporated into the strand of the gels or polymer chains. Therefore, it may be expected that the fluorescence intensity of the free pyranines should decrease as the polymerization proceeds. But, as seen from Fig. 5, the intensity of free pyranines first decreases, then makes a peak and later continues to decrease. This behavior in the fluorescence intensity of the free pyranines can be interpreted by taking into account the effect of the viscosity of polymerizing mixture.

The total intensity decreases as the number of free pyranines decreases during polymerization, but increase in the viscosity of the polymeric system can partly inhibit the mo-

tion of the pyranine, which should lead to some increase in the intensity [17–20,34,35]. These two effects together can lead the peak to appear in gelation stage. No peak appeared for low concentrated cross linked and linear polymers, since no considerable change in viscosity is observed in these cases.

One other observation is that the maxima of the short-wavelength peak (corresponding to the bonded pyranines, in Fig. 3) shifted to the relatively higher wavelengths, from 400 to 427 nm, during the polymerization process. The time elapsed for the shift from 400 to 427 nm depends on the polymer concentration. For example, it takes 240 s for $5M$, 720 s for $2M$, 1200 s for $1M$, and 1620 s for $0.1M$ (at which the gelation does not occur, a viscous solution) polymer concentrations.

The shift in wavelength from 427 to 400 nm was observed during the swelling of the gels as can be seen from Fig. 4. These shifts in wavelength of the fluorescence light during the polymerization or swelling may also give some more information about the microscopic nature of the polymer-probe interaction.

Pyranine has three functional groups which can be bonded to the polymeric network, branched or linear polymers. The probability that pyranine is bonded to the system over more than one functional group may increase with increasing polymer concentration, and also with the reaction time. As the polymerization progresses pyranine can have a chance to bind the polymeric system over two or three functional groups. Shift in the short-wavelength peak spectra from 400 to 427 nm may be due to the increasing number of the neutralized SO_3^- groups of pyranine during the polymerization. Shift from 427 to shorter wavelengths during the swelling can be interpreted by decreasing number of neutralized SO_3^- groups, some of SO_3^- bonds may be broken up upon swelling.

Figure 6 shows the fluorescence intensities from the bonded pyranine against the reaction time for some different polymer concentrations. Since the maxima of the spectra (corresponding to bonded pyranine) shifts from 400 to 427 nm as the polymerization progresses, one does not have a chance to monitor the intensity in the time drive mode of the spectrometer (10 possible data in 1 s). Therefore, we monitored the fluorescence spectra in the relatively large periods of time and plotted the intensity corresponding to the maxima of the spectra as a function of time, in Fig. 6. No considerable deviation is observed when the areas under the spectra are calculated instead of the maximum intensities. Therefore, we had the chance to get relatively more data in time, just monitoring the small part (including the maxima) of the spectra. We, then, used these data to evaluate the critical point behavior of the sol-gel transition. One can use also the continuous curves calculated by best-fitting procedure to evaluate the critical point behavior of the sol-gel transition.

Here, we would like to argue that the total fluorescence intensity from the bonded pyranines monitors the weight average degree of polymerization and the growing gel fraction for below and above the gel point, respectively. This proportionality can easily be proven by using a Stauffer-type argument [4] as follows, under the assumption that the monomers occupy the sites of an imaginary periodic lattice.

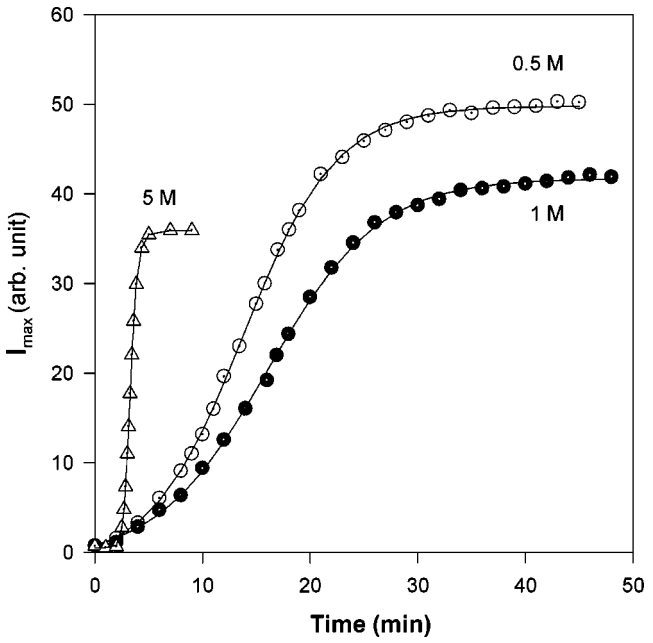

FIG. 6. Typical fluorescence intensity of the pyranine bonded to the gel for different AAm concentrations vs reaction time. The number on the curves indicates the corresponding AAm concentrations. The symbols and dashed lines represent the maximum intensity of the spectra and the best-fit lines to the experimental data, respectively.

The probability that a site belongs to a cluster of size s is given by $n_s s$, where n_s is the number of s *cluster* (number of clusters including s sites) per lattice site. The probability that an arbitrary site belongs to any cluster is p: this is simply the probability that arbitrary site is occupied. Thus, the probability w_s that the cluster to which an arbitrary occupied site belongs contains exactly s site is

$$w_s = \frac{n_s s}{\sum_s n_s s}, \tag{3}$$

and thus the average cluster size S is calculated by the following relation [3–6]:

$$S = \sum_s w_s s = \frac{\sum n_s s^2}{\sum n_s s}. \tag{4}$$

Definition of the average cluster size is the same for all dimensions, although n_s cannot be calculated exactly in higher dimensions [4]. This definition also holds for the bond percolation.

Now, let N_p be the number of pyranine molecules and N_m the other molecules (AAm, BIS, water, and APS) in the lattice. Thus, the total lattice site, N will be equal to $N_p + N_m$. The probability P_p that an arbitrary site is occupied by a pyranine molecule is simply N_p/N. The probability P_y that an arbitrary site is both a pyranine and belongs to the s cluster can be calculated as a product of w_s and P_p

TABLE I. The estimated values for the ratio C^-/C^+ (from Ref. [7]).

		Percolation			
	Classical	Direct ε expansion	$\gamma_{\varepsilon\ \mathrm{exp}}=1.840$ and $\beta_{\varepsilon\ \mathrm{exp}}=0.52$	$\gamma=1.7$ and $\beta=0.4$	Series and Monte Carlo
C^-/C^+	1	1/2.7	1/3.5	1/4.3	1/10

$$P_y = P_p w_s = \frac{P_p n_s s}{\Sigma n_s s}. \tag{5}$$

Thus, P_ys will be the total number of pyranine molecules in each cluster including s sites. The total fluorescence intensity I, which is proportional to the total number of pyranines trapped in the finite clusters, can be calculated as a summation over all s clusters

$$I \sim \sum_s P_y s = \sum_s \frac{P_p n_s s}{\sum n_s s} \cdot s = \frac{\sum P_p n_s s^2}{\sum n_s s}, \tag{6}$$

where P_p can be taken out of the summation since the concentration of the pyranine is kept fixed for our works,

$$I \sim P_p \frac{\sum n_s s^2}{\sum n_s s} = P_p S. \tag{7}$$

Thus, the last expression shows that the total normalized fluorescent intensity I is proportional to the average cluster size S. Note that the proportionality factor P_p is simply the fraction of the pyranine molecules in the sample cell. Intensity will be linearly proportional to the average cluster size, provided that the pyranine concentration is not so high to quench the fluorescence intensity by excitation transfer effect.

One important point related to Eq. (4) should be pointed out. The mean cluster size diverges if the percolation threshold is approached. This divergence is very plausible for there is an infinite cluster present above the percolation threshold then slightly below the threshold one already has very large (though finite) clusters. Thus, a suitable average over these cluster sizes is also getting very large, if one is only very slightly below the threshold. [4] The extremely large clusters in the summations, therefore, must be excluded since they disturb the average of the cluster size. This exclusion may be taken into account experimentally as coming not extremely close to the critical point, when the critical exponent γ is calculated. This effect may cause the critical region for γ to be relatively far from the critical point, as compared to β. The same problem should not occur in the calculation of the gel fraction exponent β, since it is not divergence at the threshold.

Gelation theory often makes the assumption that the conversion factor p alone determines the behavior of the gelation process, though p may depend on temperature, concentration of monomers, and time [3,4]. If the temperature and concentration are kept fixed, then p will be directly proportional to the reaction time t. This proportionality is not linear over the whole range of reaction time, but it can be assumed that in the critical region, i.e., around the critical point, $|p-p_c|$ is linearly proportional to the $|t-t_c|$ [34,35,38].

Therefore, below the gel point, i.e., for $t<t_c$, the fluorescence intensity I measures the weight average degree of polymers (or average cluster size). Above t_c, if the intensity I_{ct} from finite clusters distributed through the infinite network is subtracted from the total intensity, then, the corrected intensity $I-I_{ct}$ measures solely the gel fraction G, the fraction of the monomers that belong to the macroscopic network. In summary, we have the following relations

$$I \propto D_w^{\mathrm{pol}} = C^+ (t_c - t)^{-\gamma}, \quad t \to t_c^-, \tag{8a}$$

$$I_{ct} \propto D_w^{\mathrm{pol}} = C^- (t_c - t)^{-\gamma'}, \quad t \to t_c^+, \tag{8b}$$

$$I - I_{ct} \propto G = B(t - t_c)^{\beta}, \quad t \to t_c^+, \tag{9}$$

where C^+, C^-, and B are the critical amplitudes.

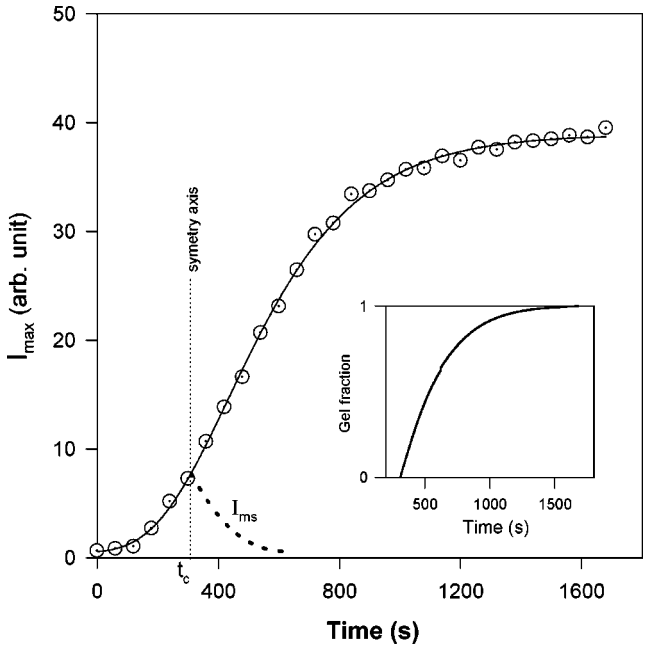

FIG. 7. A typical intensity-time curve during polymerization of AAm. The curve depicted by dots represents the mirror symmetry I_{ms} of the intensity according to the axis perpendicular to time axis at $t=t_c$. The intensity from the clusters above the gel point is calculated as $I_{ct}=(C^-/C^+)I_{ms}$. Thus, $I-I_{ct}$ monitors the growing gel fraction for $t>t_c$. The inset figure represents the gel fraction for $C^-/C^+=1$, as an example. The intensity from the lower part of the symmetry axis monitors the average cluster size for $t<t_c$.

TABLE II. Experimentally measured parameters for various AAm contents.

AAm[M]	BIS[M]	t_{gel}(s)	C^+/C^-	β	γ
5	0.032	179±5	2.7	0.47±0.02	1.80±0.05
			3.5	0.50±0.02	
			4.3	0.50±0.02	
			10	0.47±0.02	
			1.0	1.00±0.02	
3	0.019	305±5	2.7	0.50±0.02	1.80±0.05
			3.5	0.50±0.02	
			4.3	0.49±0.02	
			10	0.46±0.02	
			1.0	0.70±0.02	
2	0.013	310±5	2.7	0.52±0.02	1.70±0.05
			3.5	0.52±0.02	
			4.3	0.55±0.02	
			10	0.50±0.02	
			1.0	0.92±0.02	
1	0.0065	322±5	2.7	0.94±0.02	1.00±0.05
			3.5	0.94±0.02	
			4.3	0.95±0.02	
			10	1.00±0.02	
			1.0	0.94±0.02	
0.75	0.0048	330±5	2.7	1.00±0.02	1.00±0.05
			3.5	0.92±0.02	
			4.3	0.92±0.02	
			10	0.92±0.02	
			1.0	1.10±0.02	
0.65	0.0042	375±5	2.7	0.92±0.02	0.92±0.05
			3.5	0.92±0.02	
			4.3	0.85±0.02	
			10	0.94±0.02	
			1.0	1.03±0.02	
0.55	0.0035	872±5	2.7	0.30±0.02	
			3.5	0.29±0.02	
			4.3	0.29±0.02	
			10	0.25±0.02	
			1.0	1.00±0.02	
0.50	0.0032	1650±5	2.7	0.33±0.02	
			3.5	0.32±0.02	
			4.3	0.25±0.02	
			10	0.08±0.02	
			1.0	1.20±0.02	
0.30	0.00190	No gel			
0.10	0.00065	No gel			
0.01	0.0	No gel			

It is well known that the average cluster size of the finite clusters (distributed through the infinite network) above the gel point decreases with the same, but negative slope of the increasing cluster size before the gel point. This means that the exponents γ and γ', defined for the cluster sizes below and above the gel point, have the same values [3–6]. But the critical amplitudes for the average cluster size defined below [C^+ in Eq. (8a)] and above [C^- in Eq. (8b)] the gel point

TABLE III. Experimentally measured parameters for various BIS contents.

AAm[M]	BIS[M]	t_{gel}(s)	C^+/C^-	β	γ
1.0	0.013	222±5	2.7	1.14±0.02	0.80±0.05
			3.5	1.20±0.02	
			4.3	1.20±0.02	
			10	1.20±0.02	
			1.0	1.00±0.02	
1.0	0.019	185±5	2.7	1.15±0.02	1.00±0.05
			3.5	1.17±0.02	
			4.3	1.20±0.02	
			10	1.20±0.02	
			1.0	1.02±0.02	
1.0	0.026	195±5	2.7	1.19±0.02	0.80±0.05
			3.5	1.10±0.02	
			4.3	1.17±0.02	
			10	1.17±0.02	
			1.0	1.01±0.02	
1.0	0.032	163±5	2.7	1.20±0.02	0.90±0.05
			3.5	1.40±0.02	
			4.3	1.40±0.02	
			10	1.40±0.02	
			1.0	1.00±0.02	

are different, and there exists a universal value for the ratio C^+/C^-. This ratio is different for mean field versus percolation as discussed by Aharony [7] and Stauffer [3]. The estimated values for C^+/C^- [3,7] is given in Table I.

To determine the intensity I_{ct} in Eqs. (8b) and (9), we first

TABLE IV. Experimentally measured parameters for different temperatures.

AAm[M]	T (°C)	t_{gel}(s)	C^+/C^-	β	γ
1.0	35	125±5	2.7	1.17±0.02	0.80±0.05
			3.5	1.15±0.02	
			4.3	1.15±0.02	
			10	1.20±0.02	
			1.0	1.00±0.02	
1.0	40	112±5	2.7	1.20±0.02	1.00±0.05
			3.5	1.20±0.02	
			4.3	1.25±0.02	
			10	1.25±0.02	
			1.0	1.01±0.02	
1.0	45	195±5	2.7	0.80±0.02	1.02±0.05
			3.5	0.90±0.02	
			4.3	0.90±0.02	
			10	0.85±0.02	
			1.0	1.00±0.02	
1.0	50	163±5	2.7	0.80±0.02	1.00±0.05
			3.5	0.70±0.02	
			4.3	0.75±0.02	
			10	0.75±0.02	
			1.0	1.00±0.02	

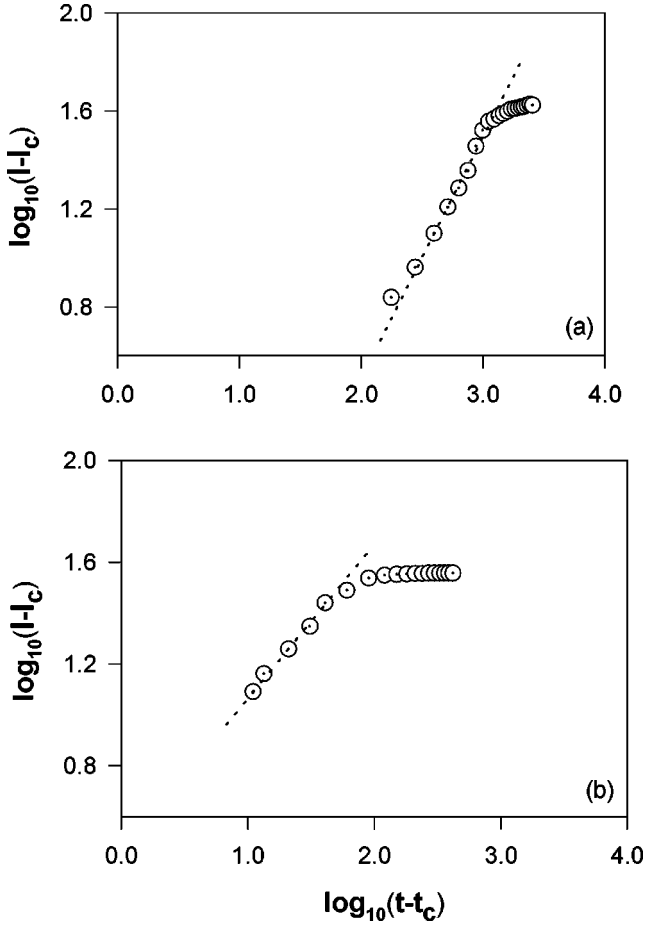

FIG. 8. Double logarithmic plot of the intensity $I-I_{ct}$ vs time curves above t_c for $1M$ and $5M$ AAm concentrations. The β exponents were determination from the slope of the straight lines near the gel points. As seen, the scaling region comes closer to the critical point as the AAm concentration is increased.

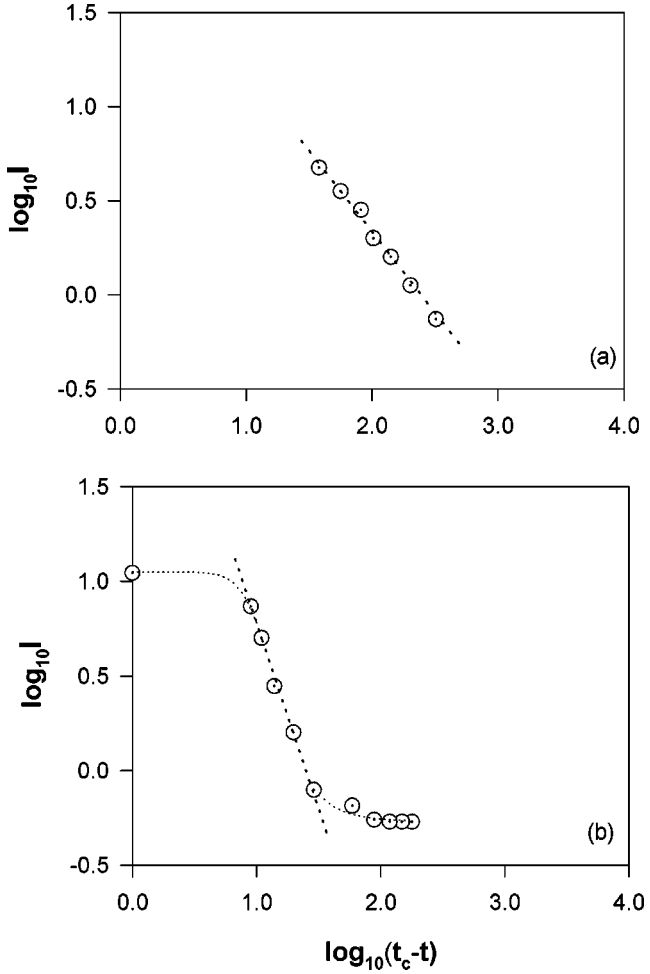

FIG. 9. Double logarithmic plot of the intensity vs time for $t<t_c$. The γ exponents were determination from the slope of the straight lines near the gel points. As seen, the scaling region comes closer to the critical point as the AAm concentration is increased, as in the case for β.

choose the parts of the intensity-time curve up to the gel points, then the mirror symmetry I_{ms} of these parts according to the axis perpendicular to time axis at the gel point were multiplied by the ratio C^-/C^+, so that $I_{ct}=(C^-/C^+)I_{ms}$. Thus, I_{ct} measures solely the intensity from the cluster above the gel point, and $I-I_{ct}$ measures the intensity from the gel fraction. This process is clarified explicitly in Fig. 7.

Using Eqs. (8) and (9), and the values for t_c summarized in Tables II, III, and IV, we calculated γ and β exponents as function of AAm concentration, BIS concentration, and temperature. Figures 8 and 9 represent the log-log plots of some typical intensity-time data above and below the gel point, where the slope of the straight lines, close to the gel points, give β and γ exponents, respectively.

The concentration and C^-/C^+ dependence of the exponents are summarized in Table II, where three distinct concentration regimes appear. In the lowest concentration regime the exponents β and γ obey neither the percolation nor the classical theory. In the intermediate regime, they have the values close to unity, which agree with the classical theory independent of C^-/C^+. Finally, for the highest concentration regime they obey the percolation results in the experimental range of errors when C^-/C^+ has the percolation values. The observation of three regimes of behavior was also previously observed by Rubinstein and Colby [39] for modulus G_0 of gels and maximum swelling Q, as a function of the proximity to the gel point ε.

IV. CONCLUSION

The application of fluorogenic probe molecules for *in situ* monitoring of free radical cross-linking polymerization is illustrated by measuring the polymerization of AAm. The probe molecules fluoresce at different wavelengths when they are incorporated into growing polymer chains. The fluorescence intensity from the bonded probes is therefore a measure of the degree of polymerization and gel fraction at below and above the gel point. In this study, we report on a method to examine the percolation picture of gelation in an unequivocal way. We are, thus, able to measure directly polymerization kinetics without disturbing the system mechanically, and to test the universality of the sol-gel transition as a function of the parameters such as polymer concentration,

cross-linker concentration, and temperature.

The gel fraction exponent β and the average cluster size exponent γ agree best with the Flory-Stockmayer theory in the concentration range of $0.65M$ to $1M$ independent of the ratio C^-/C^+, and agree with percolation theory for higher AAm concentrations above $1M$ when the ratio C^-/C^+ takes the values given in the percolation theory.

It seems that this crossover from mean field to the percolation is related to the fact that we are able only to approach the critical point to $|p-p_c/p_c| \geqslant 0.1$ for the concentrations below $2M$ of AAm, as can be calculated easily from Figs. 8 and 9. Above $1M$ of AAm, it seems we are able to approach the true critical region where $|p-p_c/p_c| \geqslant 0.01$.

An experimental system with intermediate N will exhibit a crossover between mean-field behavior, far from the gel point, and critical behavior, close to the percolation threshold, in a manner similar to other continuous phase transitions [9,40]. For large N the critical region in which the exponents are calculated is quite small. Thus, the entire range of experimentally accessible $|p-p_c|$ will be in the mean-field class, and modeled by the Flory-Stockmayer theory [1,2].

To check whether the apparent mean-field behavior is due to measurements that might have been made outside the true critical region, we repeated some of the experiments both without TEMED (radical polymerization) at the temperatures of 55, 60, 65, 70, and 75 °C and with extremely small amount of TEMED at room temperature to slow down the gelation kinetics. The effect of the TEMED on the hydrolysis of PAAm gel was previously investigated by Shibayama *et al.* [41] They investigated that TEMED triggers hydrolysis of PAAm gels.

The results showed that the exponents do not differ seriously for the samples without TEMED above room temperature. But, the sample for $5M$ AAm including extremely small amount of TEMED, at room temperature (the reaction takes about 250 min) showed some considerable difference for β exponent. It is observed that the bigger the value of C^-/C^+ (the smaller C^+/C^-), the better the β exponent agrees with the percolation result. Here, it should be noted that it was not possible to carry out the polymerization at room temperature without TEMED. To be able to perform the reaction either you have to add some TEMED to the prepolymerization solution, even if the content of the TEMED is extremely small, or the reaction must be carried out above higher temperatures.

The dependency of the β exponent to the choice of C^-/C^+, for the samples including extremely small amount of TEMED at room temperature, needs do be investigated by careful experiments. Here it is important to note that β exponent agrees better to the percolation theory when the value of C^-/C^+ is increased (C^+/C^- is decreased). This point supports the study of Aharony [7] where it is indicated that C^+/C^- should agree best with ε-expansion estimates (see Table I).

It seems that 0.65 and $2M$ concentrations are crossover concentrations for γ and β exponents; $0.65M$ from nonuniversal to mean field, and $2M$ from mean field to percolation values for acrylamide system. Ginzburg criterion [9] becomes true for $2M$ AAm. The nonuniversal behavior for extremely small concentrations may be due to the fact that we are extremely far away from the critical region for these experimental conditions.

ACKNOWLEDGMENT

Y.Y. has been supported by the Turkish Academy of Sciences (TUBA) (Grant No. EA-TUBA-GEBIP/2001-1-1).

[1] P. J. Flory, J. Am. Chem. Soc. **63**, 3083 (1941); **63**, 3091 (1941); **63**, 3096 (1941).
[2] W. Stockmayer, J. Chem. Phys. **11**, 45 (1943); **12**, 125 (1944).
[3] D. Stauffer, A. Coniglio, and M. Adam, Adv. Polym. Sci. **44**, 193 (1982).
[4] D. Stauffer and A. Aharony *Introduction to Percolation Theory* 2nd ed. (Taylor and Francis, London, 1994).
[5] M. Sahimi, *Application of Percolation Theory* (Taylor and Francis, London, 1994).
[6] P. G. de Gennes, *Scaling Concepts in Polymer Physics* (Cornell University Press, Ithaca, NY, 1988), p. 54.
[7] A. Aharony, Phys. Rev. B **22**, 400 (1980).
[8] R. H. Colby and M. Rubinstein, Phys. Rev. E **48**, 3712 (1993).
[9] C. P. Lusignan, T. H. Mourey, J. C. Wilson, and R. H. Colby, Phys. Rev. E **60**, 5657 (1999).
[10] (a) Y. Liu and R. B. Pandey, J. Chem. Phys. **105**, 825 (1996); (b) R. B. Pandey and Y. Liu, J. Sol-Gel Sci. Technol. **15**, 147 (1999).
[11] G. M. Barrow, *Introduction to Molecular Spectroscopy* (McGraw-Hill, New York, 1962).
[12] J. B. Birks, *Photophysics of Aromatic Molecules* (Wiley, London, 1965).
[13] *Fluorescence and Phosphorescence Analysis*, edited by D. M. Herculus (Wiley, New York, 1965).
[14] M. D. Galanin, *Luminescence of Molecules and Crystals* (Cambridge International Science, Cambridge, 1995).
[15] W. F. Jager, A. A. Volkers, and D. C. Neckers, Macromolecules **28**, 8153 (1995).
[16] T. C. Schaeken and J. M. Warman, J. Phys. Chem. **99**, 6145 (1995).
[17] J. S. Royal and J. M. Torkelson, Macromolecules **26**, 5331 (1993).
[18] K. E. Miller, R. H. Krueger, and J. M. Torkelson, J. Polym. Sci., Part B: Polym. Phys. **33**, 2343 (1995).
[19] R. Vatanparast, S. Li, K. Hakala, and H. Lemmetyinen, Macromolecules **33**, 438 (2000).
[20] J. M. Warman, R. D. Abellon, H. J. Verhey, J. W. Verhoeven, and J. W. Hofstraat, J. Phys. Chem. B **101**, 4913 (1997).
[21] Ş. Erçelen, A. S. Klymchenko, and A. P. Demchenko, Anal. Chim. Acta **464**, 273 (2002).
[22] W. F. Jager, A. M. Sarker, and D. C. Neckers, Macromolecules **32**, 8791 (1999).
[23] Ö. Pekcan, Y. Yılmaz, and O. Okay, Polymer **38**, 1693 (1997).
[24] Y. Yılmaz, Y. Yagcı, and Ö. Pekcan, J. Macromol. Sci., Pure Appl. Chem. **A38**, 741 (2001).

[25] Ö. Pekcan, Y. Yılmaz, and O. Okay, Chem. Phys. Lett. **229**, 537 (1994).
[26] B. Serrano, B. Levenfeld, J. Bravo, and J. Baselga, Polym. Eng. Sci. **36**, 175 (1996).
[27] O. Okay, Y. Yılmaz, D. Kaya, M. Keskinel, and Ö. Pekcan, Polym. Bull. (Berlin) **43**, 425 (1999).
[28] Ö. Pekcan and Y. Yılmaz, J. Appl. Polym. Sci. **63**, 1777 (1997).
[29] Ö. Pekcan, Y. Yılmaz, and Ş. Uğur, Polym. Int. **44**, 474 (1997).
[30] Y. Yılmaz and Ö. Pekcan, Polymer **39**, 5351 (1998).
[31] O. Guney, Y. Yılmaz, and Ö. Pekcan, Sens. Actuators B **85**, 86 (2002).
[32] T. Oya, T. Enoki, A. Yu. Grosberg, S. Masamune, T. Sakiyama, Y. Takeoka, K. Tanaka, G. Wang, Y. Yılmaz, M. S. Feld, R. Dasari, and T. Tanaka, Science **286**, 1543 (1999).
[33] Y. Yılmaz, Phys. Rev. E **66**, 05801 (2002).
[34] Y. Yılmaz, A. Erzan, and Ö. Pekcan, Eur. Phys. J. E **9**, 135 (2002).
[35] Y. Yılmaz, A. Erzan, and Ö. Pekcan, Phys. Rev. E **58**, 6 (1998).
[36] A. Pagnoni, A. M. Kligman, and T. Stoudemayer, J. Cosmet. Sci., **49**, 33 (1998).
[37] O. Okay, D. Kaya, and Ö. Pekcan, Polymer **40**, 6179 (1999).
[38] E. Tuzel, M. Özmetin, Y. Yılmaz, and Ö. Pekcan, Eur. Polym. J. **36**, 727 (2000).
[39] M. Rubinstein and R. H. Colby, Macromolecules **27**, 3184 (1994).
[40] R. H. Colby *et al.*, Macromolecules **25**, 7180 (1992).
[41] S. Tanaka, T. Norisuye, and M. Shibiyama, Macromolecules **32**, 3989 (1999).